

Matter-waves in Bose-Einstein condensates with spin-orbit and Rabi couplings

Emerson Chiquillo

Escuela de Física, Universidad Pedagógica y Tecnológica de Colombia (UPTC),
Avenida Central del Norte, Tunja, Colombia.

E-mail: emerson.chiquillo@uptc.edu.co

Abstract. We investigate the one-dimensional (1D) and two-dimensional (2D) reduction of a quantum field theory starting from the three-dimensional (3D) many-body Hamiltonian of interacting bosons with spin-orbit (SO) and Rabi couplings. We obtain the effective time-dependent 1D and 2D nonpolynomial Heisenberg equations for both repulsive and attractive signs of the inter-atomic interaction. Our findings show that in case in which the many-body state coincides with the Glauber coherent state, the 1D and 2D Heisenberg equations become 1D and 2D nonpolynomial Schrödinger equations (NPSEs). These models were derived in a mean-field approximation from 3D Gross-Pitaevskii equation (GPE), describing a Bose-Einstein condensate (BEC) with SO and Rabi couplings. In the present work self-repulsive and self-attractive localized solutions of the 1D NPSE and the 1D GPE are obtained in a numerical form. The combined action of SO and Rabi couplings produces conspicuous sidelobes on the density profile, for both signs of the interaction. In the case of the attractive nonlinearity, an essential result is the possibility of getting an unstable condensate by increasing of SO coupling.

PACS numbers: 03.70.+k, 67.85.-d, 03.75.Mn, 67.85.Hj

1. Introduction

In last two decades, the ultracold atomic gases have provided an important environment for studying quantum many-particle systems from the experimental realization and the theoretical viewpoint. In last few years, the huge interest in the ultracold gases field has allowed the experimental realization of an artificial spin-orbit (SO) coupling in a neutral atomic Bose-Einstein condensate (BEC) by means of counterpropagating laser beams which couple two atomic spin states [1, 2]. The SO coupling has been also created in fermionic atomic gases [3, 4]. These experimental breakthroughs have led to significant theoretical works, opening the door to a fascinating and fast developing on SO coupled cold atoms research.

Basic theoretical and experimental aspects on SO coupled degenerate atomic gases are introduced in the reviews [5, 6]. The theoretical activities have been devoted to the SO coupled Bose-Einstein condensates (BECs) among others, including vortex in rotating SO coupled BECs [7, 8, 9, 10]. Trapped two-dimensional (2D) atomic BECs with spin-independent interactions in the presence of isotropic SO coupling [11, 12]. In a two-component Bose gas confined in a 2D harmonic oscillator (HO) potential, with an isotropic SO coupling Rashba type, the ground state has a half-quantum angular momentum vortex configuration [13]. The ground-state properties of a weakly trapped spin-1 BEC with SO coupling were studied by means of numerical and analytical methods in an external Zeeman field [14]. From numerical simulation spin-1/2 and spin-1 BECs with Rashba SO coupling were studied [15], identifying two different phases. In one phase, the ground state is a single plane wave. In the other phase, the condensate wave function is a standing wave, and it forms a spin stripe. In [16], low-energy stationary states of pseudospin-1 BECs in the presence of Rashba-Dresselhaus-type SO coupling were numerically investigated. The quantum tricriticality and phase transitions in SO coupled BECs were studied by considering a SO coupled configuration of spin-1/2 interacting bosons with equal Rashba and Dresselhaus couplings in a mean-field approximation [17]. In [18] were studied isotropically interacting bosons with Rashba SO coupling. The bosons condenses into a single momentum state of the Rashba spectrum via the mechanism of order by disorder. The existence of antiferromagnetically ordered (striped) ground states in a 1D SO coupled system with repulsive atomic interactions under the presence of a trapping HO it was demonstrated in [19]. An experimental scheme to create SO coupling in spin-3 Cr atoms using Raman processes was proposed, and the ground-state structures of a SO coupled Cr condensate were studied [20]. Thus showing, in addition to the stripe structures induced by the SO coupling, the magnetic dipole-dipole interaction gives rise to the vortex phase, in which a spontaneous spin vortex is formed. Solitons in a BEC with SO coupling were introduced in 1D geometries [21, 22, 23, 24] and 2D geometries [25, 26, 27]. Vortex-lattice solutions to the coupled mean-field equations with the SO coupling and optical lattice (OL) potential were reported in [28]. Vortex dynamics in SO coupled BECs was studied in [29, 30]. In [31] it was carried out a study by means of a variational approximation and numerical

solutions of localization of a noninteracting and weakly interacting SO coupled BEC in a quasiperiodic bichromatic OL potential, confirming the existence of stationary localized states in the presence of the SO and Rabi couplings for equal numbers of atoms in the two components. The stability of plane waves in a 2D SO coupled BEC was studied analytically in [32, 33]. Recently, has been studied the formation of bound states and three-component bright vector solitons in a quasi-1D SO coupled hyperfine spin $f = 1$ BEC and the five component vector solitons in a quasi-1D SO coupled hyperfine spin-2 BEC using a numerical solution and a variational approximation of a mean-field model [34, 35]. It was considered a theory of collapse in BECs with inter-atomic attraction for two different realizations of SO coupling [36], the axial Rashba coupling and the balanced effectively 1D Rashba-Dresselhaus coupling. The spin-dependent anomalous velocity in Rashba coupled BECs forms a centrifugal component in the density flux opposite to that arising due to the attraction between particles and prevents the collapse at a sufficiently strong coupling. In BECs with balanced Rashba-Dresselhaus coupling, the spin-dependent velocity can spatially split the initial state in 1D and form spin-projected wavepackets, reducing the total condensate density. The quantum dynamics of a SO coupled BEC in a double-well potential was investigated in [37]. It was found that the SO coupling can significantly enhance the atomic interwell tunneling. By employing the two-mode approximation from mean-field GPE and numerical methods, the Josephson oscillations of SO coupled BECs were studied in [38]. This was carried out by analyzing the interplay between the inter-atomic interactions and the SO coupling and the self-trapped dynamics of the inter-species imbalance.

In the ultracold bosonic gases context at zero temperature, a good theoretical tool for researching on dynamics of dilute BECs is the time-dependent mean-field 3D GPE [40]. An interesting theoretical problem is the derivation of reduced 1D and 2D models to studying the behavior of these systems. Experimentally these effective models are an ideal platform for testing many-body phenomena [39, 41, 42, 43]. Theoretically they have been adopted various approaches to derive effective 1D and 2D reduced equations from the 3D GPE [44, 45]. Being this latest work the most applicable describing the dynamics of BECs. Some examples of 1D and 2D reduction for studying BECs with a non-local dipolar interaction in a mean-field approximation are given in [46]. A starting point for the theoretical study of SO coupled BECs in reduced dimensionality is provided by a binary mean-field nonpolynomial Schrödinger equation (NPSE), which is derived in [24]. The system of coupled equations was used to investigate localized modes in dense repulsive and attractive BECs with the SO and Rabi couplings. Recently, it was considered an effectively 2D BEC with the SO coupling of mixed Rashba-Dresselhaus type and Rabi term [27]. The system is described by two coupled 2D NPSEs, for both attractive and repulsive inter-atomic interactions. Approximate localized solutions are analyzed by treating the SO and Rabi terms as perturbations. Localized solutions of the system are obtained in a numerical form. There have also been theoretical efforts toward understanding the physics of the SO coupled Bose gases at finite temperature [47]. Here it was found that in three spatial dimensions SO coupling lowers the critical

temperature of condensation and enhances thermal depletion of the condensate fraction. In two dimensions the SO coupling destroys superfluidity at any finite temperature.

In this paper, starting from the 3D many-body Hamiltonian describing N interacting bosons with SO and Rabi couplings and where the dynamics is ruled by two coupled field equations, we investigate the 1D and 2D reduction of a bosonic quantum field theory. In the derivation of the 1D model we use a transverse and isotropic harmonic confinement and a generic trapping potential in the axial direction. In the 2D system the trapping potential is harmonic in the axial direction and generic in the transverse one. We achieve to getting reduced models of time-dependent 1D and 2D nonpolynomial Heisenberg coupled equations. The derivation is performed for both the repulsive and attractive signs of the inter-atomic, intra- and inter-species interactions. In the case which the many-body quantum state of the system coincides with the Glauber coherent state our findings agree with the two coupled NPSEs in 1D [24] and 2D [27]. The derivation of the effective equations is followed by the numerical analysis of new features of trapped modes in the 1D NPSE and 1D GPE describing the dynamics of a BEC with SO and Rabi couplings, for both signs of the nonlinearity.

The rest of the paper is organized in the following way. In the Sec. 2, we derive an effective 1D nonpolynomial Heisenberg equation. This section also includes the condition under which the Heisenberg equation coincides with the 1D NPSE describing a BEC with SO and Rabi couplings. The 2D reduction of the 3D Hamiltonian is presented in Sec. 3. Numerical results of the 1D NPSE and 1D GPE are reported in Sec. 4. Finally, we present a summary and discussion of our study in Sec. 5.

2. Dimensional reduction of a quantum field theory

A quantum treatment of interacting bosons with SO and Rabi couplings can be obtained starting from the many-body Hamiltonian in second quantization, which describes N interacting bosons of equal mass m confined by an external potential $U(\mathbf{r})$,

$$\begin{aligned} \hat{H} = & \int d\mathbf{r} \hat{\Psi}^\dagger(\mathbf{r}) H_{sp} \hat{\Psi}(\mathbf{r}) \\ & + \frac{1}{2} \int d\mathbf{r} \hat{\Psi}^\dagger(\mathbf{r}) \hat{\Psi}^\dagger(\mathbf{r}') V(\mathbf{r} - \mathbf{r}') \hat{\Psi}(\mathbf{r}') \hat{\Psi}(\mathbf{r}) \end{aligned} \quad (1)$$

where $\hat{\Psi}^\dagger(\mathbf{r})$ and $\hat{\Psi}(\mathbf{r})$ are the two pseudo-spin creation and annihilation boson field operators, respectively. Thus, $\hat{\Psi} = (\hat{\psi}_1, \hat{\psi}_2)^T$ and $\hat{\Psi}^\dagger = (\hat{\psi}_1^\dagger, \hat{\psi}_2^\dagger)$. The term $V(\mathbf{r} - \mathbf{r}')$ stands for the two-body interaction. The single-particle SO Hamiltonian H_{sp} [24] is,

$$H_{sp} = \left[\frac{\hat{\mathbf{p}}^2}{2m} + U(\mathbf{r}) \right] \sigma_0 + \frac{\hbar\Omega}{2} \sigma_x - \frac{k_L}{m} \hat{p}_x \sigma_z \quad (2)$$

where $\hat{\mathbf{p}}^2 = -\hbar^2 \nabla^2$ is the square of the momentum operator, $U(\mathbf{r})$ is a trapping potential, Ω is the frequency of the Raman coupling, which is responsible for the Rabi mixing between the two states, k_L is the recoil wave number induced by the interaction with the laser beams, σ_0 is the two-dimensional unit matrix and $\sigma_{x,z}$ are the Pauli

matrices. By assuming a dilute system of bosons, the inter-particle interaction can be approximate by a contact pseudo-potential. We consider interactions for both intra- and inter-species. This means that the potential for intra-species interactions is assumed as $V(\mathbf{r} - \mathbf{r}') \equiv (4\pi\hbar^2 a_{jj}/m)\delta(\mathbf{r} - \mathbf{r}')$, where $4\pi\hbar^2 a_{jj}/m$ is the strength of interaction, a_{jj} is the intra-species s-wave scattering length with $j = 1, 2$ for the two pseudo-spin components. In the inter-species interactions the potential has the same form, but the strength of the interaction takes the form $4\pi\hbar^2 a_{12}/m$. In order to transform the Hamiltonian (1) into dimensionless form, we use the HO length of the transverse trap $a_\perp = \sqrt{\hbar/(m\omega_\perp)}$, with the trapping frequency ω_\perp . The time t is measured in units of ω_\perp^{-1} , the spatial variable \mathbf{r} in units of a_\perp , the energy in units $\hbar\omega_\perp$ and the field operators are given in units of $a_\perp^{3/2}$. By using these new variables we have the dimensionless many-body Hamiltonian in second quantization,

$$\hat{H} = \hat{H}_{sp} + \hat{H}_{int} \quad (3)$$

where,

$$\begin{aligned} \hat{H}_{sp} = \int d\mathbf{r} \left\{ \sum_{j=1,2} \hat{\psi}_j^\dagger \left[-\frac{1}{2}\nabla^2 + U(\mathbf{r}) \right. \right. \\ \left. \left. + (-1)^{j-1} i\gamma \frac{\partial}{\partial x} \right] \hat{\psi}_j + \Gamma(\hat{\psi}_1^\dagger \hat{\psi}_2 + \hat{\psi}_2^\dagger \hat{\psi}_1) \right\} \end{aligned} \quad (4)$$

and

$$\hat{H}_{int} = \int d\mathbf{r} \left[\sum_{j=1,2} \pi g_{jj} \hat{\psi}_j^\dagger \hat{\psi}_j^\dagger \hat{\psi}_j \hat{\psi}_j + 2\pi g_{12} \hat{\psi}_1^\dagger \hat{\psi}_2^\dagger \hat{\psi}_2 \hat{\psi}_1 \right] \quad (5)$$

where $j = (1, 2)$ and ψ_j represents the field operators of the two atomic states, $g_{jj} \equiv 2a_{jj}/a_\perp$, $g_{12} \equiv 2a_{12}/a_\perp$ are the strengths of the intra- and inter-species interactions. $\gamma \equiv k_L a_\perp$ and $\Gamma \equiv \Omega/(2\omega_\perp)$ are dimensionless strengths of the SO and Rabi couplings, respectively. The external potential is given as $U(\mathbf{r}) = V(x) + (y^2 + z^2)/2$. Thus, the many-body Hamiltonian (3) describes a dilute gas of bosonic atoms with SO and Rabi couplings confined in the transverse (y, z) plane by a HO potential and a generic potential $V(x)$ in the x axial direction. The bosonic field operator $\hat{\psi}(\mathbf{r}, t)$ and its adjoint $\hat{\psi}^\dagger(\mathbf{r}, t)$ must satisfy the following equal-time commutation rules

$$[\hat{\psi}_\alpha(\mathbf{r}, t), \hat{\psi}_\beta^\dagger(\mathbf{r}', t)] = \delta(\mathbf{r} - \mathbf{r}')\delta_{\alpha\beta} \quad (6)$$

$$[\hat{\psi}_\alpha(\mathbf{r}, t), \hat{\psi}_\beta(\mathbf{r}', t)] = [\hat{\psi}_\alpha^\dagger(\mathbf{r}, t), \hat{\psi}_\beta^\dagger(\mathbf{r}', t)] = 0 \quad (7)$$

where $\alpha, \beta = 1, 2$. By imposing these commutation rules we find the creation of a particle in the state $|\mathbf{r}, \alpha, t\rangle$ from the vacuum state $|0\rangle$ as, $\hat{\psi}_\alpha^\dagger(\mathbf{r}, t)|0\rangle = |\mathbf{r}, \alpha, t\rangle$. The annihilation of a particle, which is in the state $|\mathbf{r}, \beta, t\rangle$ is given by $\hat{\psi}_\alpha(\mathbf{r}', t)|\mathbf{r}, \beta, t\rangle = \delta(\mathbf{r} - \mathbf{r}')\delta_{\alpha\beta}|0\rangle$. From the Heisenberg equation of motion

$$i\frac{\partial \hat{\Psi}}{\partial t} = [\hat{\Psi}, \hat{H}] \quad (8)$$

we get two coupled field equations in a closed form,

$$\begin{aligned} i\frac{\partial}{\partial t}\hat{\psi}_j(\mathbf{r}, t) = & \left[-\frac{1}{2}\nabla^2 + V(x) + \frac{1}{2}(y^2 + z^2) \right. \\ & + (-1)^{j-1}i\gamma\frac{\partial}{\partial x} + 2\pi g_{jj}\hat{\psi}_j^\dagger(\mathbf{r}, t)\hat{\psi}_j(\mathbf{r}, t) \\ & \left. + 2\pi g_{12}\hat{\psi}_{3-j}^\dagger(\mathbf{r}, t)\hat{\psi}_{3-j}(\mathbf{r}, t) \right] \hat{\psi}_j(\mathbf{r}, t) + \Gamma\hat{\psi}_{3-j}(\mathbf{r}, t) \end{aligned} \quad (9)$$

2.1. 1D-reduction of the 3D-Hamiltonian

To perform the one-dimensional reduction of the 3D Hamiltonian (3) we suppose that in the transverse (y, z) plane the single-particle ground-state is a Gaussian wave-function [48, 49, 50] as in a BEC. Thus

$$\hat{\psi}_j(\mathbf{r})|G\rangle = \frac{1}{\sqrt{\pi}\eta_j(x, t)} \exp\left[-\frac{y^2 + z^2}{2\eta_j^2(x, t)}\right] \hat{\phi}_j(x, t)|G\rangle \quad (10)$$

where $|G\rangle$ is the many-body ground state, while $\eta_j(x, t)$ is the transverse width for bosonic field operators and $\hat{\phi}_j(x, t) = (\hat{\phi}_1(x, t), \hat{\phi}_2(x, t))^T$ represents the axial bosonic field operators. By applying this ansatz into the Hamiltonian (3), we obtain the effective Hamiltonian \hat{h}_{1D} such that

$$\hat{H}|G\rangle = \hat{h}_{1D}|G\rangle \quad (11)$$

Neglecting the space derivatives of $\eta_j(x, t)$, the effective 1D-Hamiltonian can be read

$$\begin{aligned} \hat{h}_{1D} = & \int dx \left\{ \sum_{j=1,2} \hat{\phi}_j^\dagger \left[-\frac{1}{2}\frac{\partial^2}{\partial x^2} + V(x) + \frac{1}{2}\left(\frac{1}{\eta_j^2} + \eta_j^2\right) \right. \right. \\ & + (-1)^{j-1}i\gamma\frac{\partial}{\partial x} + \frac{g_{jj}}{2\eta_j^2}\hat{\phi}_j^\dagger\hat{\phi}_j \left. \right] \hat{\phi}_j + \frac{2g_{12}}{\eta_1^2 + \eta_2^2}\hat{\phi}_1^\dagger\hat{\phi}_2^\dagger\hat{\phi}_2\hat{\phi}_1 \\ & \left. + 2\Gamma\frac{\eta_1\eta_2}{\eta_1^2 + \eta_2^2} \sum_{j=1,2} \hat{\phi}_j^\dagger\hat{\phi}_{3-j} \right\} \end{aligned} \quad (12)$$

The ground state $|G\rangle$ is obtained self-consistently from the Hamiltonian (12) and the transverse width $\eta_j(x, t)$. It is determined by minimizing the energy functional $\langle G|\hat{h}|G\rangle$ with respect to $\eta_j(x, t)$. In this way we get

$$\begin{aligned} \eta_j^4 = & 1 + g_{jj}\frac{\langle G|\hat{\phi}_j^\dagger\hat{\phi}_j^\dagger\hat{\phi}_j\hat{\phi}_j|G\rangle}{\langle G|\hat{\phi}_j^\dagger\hat{\phi}_j|G\rangle} + 4g_{12}\frac{\eta_j^4}{(\eta_1^2 + \eta_2^2)^2}\frac{\langle G|\hat{\phi}_1^\dagger\hat{\phi}_2^\dagger\hat{\phi}_2\hat{\phi}_1|G\rangle}{\langle G|\hat{\phi}_j^\dagger\hat{\phi}_j|G\rangle} \\ & + 2\Gamma(-1)^{j-1}\eta_j^3\eta_{3-j}\frac{\eta_1^2 - \eta_2^2}{(\eta_1^2 + \eta_2^2)^2}\frac{\langle G|(\hat{\phi}_1^\dagger\hat{\phi}_2 + \hat{\phi}_2^\dagger\hat{\phi}_1)|G\rangle}{\langle G|\hat{\phi}_j^\dagger\hat{\phi}_j|G\rangle} \end{aligned} \quad (13)$$

The 1D-Hamiltonian \hat{h}_{1D} (12), is a generalization of the one introduced by Salasnich [49], in the context of a BEC in presence of an axial potential. In the case which the SO and Rabi couplings are dropped the effective Hamiltonian \hat{h}_{1D} corresponds with the model implemented in [49].

2.2. 1D-nonpolynomial Heisenberg equation

From the effective 1D-Hamiltonian (12) and the Heisenberg equation of motion

$$i\frac{\partial}{\partial t}\hat{\phi}_j = [\hat{\phi}_j, \hat{h}_{1D}] \quad (14)$$

we derive the 1D-nonpolynomial Heisenberg equation, which represents the motion of a many-body quantum system of dilute bosonic atoms,

$$\begin{aligned} i\frac{\partial}{\partial t}\hat{\phi}_j = & \left[-\frac{1}{2}\frac{\partial^2}{\partial x^2} + V(x) + \frac{1}{2}\left(\frac{1}{\eta_j^2} + \eta_j^2\right) + (-1)^{j-1}i\gamma\frac{\partial}{\partial x} + \frac{g_{jj}}{\eta_j^2}\hat{\phi}_j^\dagger\hat{\phi}_j \right. \\ & \left. + \frac{2g_{12}}{\eta_1^2 + \eta_2^2}\hat{\phi}_{3-j}^\dagger\hat{\phi}_{3-j} \right]\hat{\phi}_j + 2\Gamma\frac{\eta_1\eta_2}{\eta_1^2 + \eta_2^2}\hat{\phi}_{3-j} \end{aligned} \quad (15)$$

This equation must be solved self-consistently by using the many-body quantum state of the system $|S\rangle$ in the equations of the transverse widths η_j . So

$$\begin{aligned} \eta_j^4(x, t) = & 1 + g_{jj}\frac{\langle S|\hat{\phi}_j^\dagger(x, t)\hat{\phi}_j^\dagger(x, t)\hat{\phi}_j(x, t)\hat{\phi}_j(x, t)|S\rangle}{\langle S|\hat{\phi}_j^\dagger(x, t)\hat{\phi}_j(x, t)|S\rangle} \\ & + 4g_{12}\frac{\eta_j^4}{(\eta_1^2 + \eta_2^2)^2}\frac{\langle S|\hat{\phi}_1^\dagger(x, t)\hat{\phi}_2^\dagger(x, t)\hat{\phi}_2(x, t)\hat{\phi}_1(x, t)|S\rangle}{\langle S|\hat{\phi}_j^\dagger(x, t)\hat{\phi}_j(x, t)|S\rangle} \\ & + 2\Gamma(-1)^{j-1}\eta_j^3\eta_{3-j}\frac{\eta_1^2 - \eta_2^2}{(\eta_1^2 + \eta_2^2)^2} \\ & \times \frac{\langle S|(\hat{\phi}_1^\dagger(x, t)\hat{\phi}_2(x, t) + \hat{\phi}_2^\dagger(x, t)\hat{\phi}_1(x, t))|S\rangle}{\langle S|\hat{\phi}_j^\dagger(x, t)\hat{\phi}_j(x, t)|S\rangle} \end{aligned} \quad (16)$$

In an open environment particles may be added or removed from the condensate, and one can suppose that the number of bosons in the matter field is not fixed. This implies that the condensate is not in a pure Fock state [50, 51, 52]. We then introduce, in analogy with optics the Glauber coherent states $|GCS\rangle$ [53], which do not have a fixed number of particles. On the other hand, the interacting many-body system described with quantum field theory is equivalent to an infinite number of interacting harmonic oscillators. As an useful ingredient in the functional formulation of quantum field theory [51], it is possible introduce the coherent states in the familiar setting of a single harmonic oscillator. In this theory, the partition function is writing as a functional integral over time-dependent fields, which are the eigenvalues of the coherent states. The Glauber coherent state $|GCS\rangle$, is introduced as the eigenstate of the annihilation operator. In terms of quantum field operators we have $\hat{\phi}_j(x, t)|GCS\rangle = \phi_j(x, t)|GCS\rangle$ where $j = 1, 2$ and $\phi_j(x, t)$ is a classical field. The average number of atoms in the coherent state is given by $N_j = \langle GCS|\hat{N}_j|GCS\rangle$. Hence in the case in which the many-body state $|S\rangle$ coincides with the Glauber coherent state $|GCS\rangle$ [48, 49], the 1D-nonpolynomial Heisenberg equation (15) becomes 1D-nonpolynomial Schrödinger equation describing a BEC with SO and Rabi couplings

$$i\frac{\partial}{\partial t}\phi_j = \left[-\frac{1}{2}\frac{\partial^2}{\partial x^2} + V(x) + \frac{1}{2}\left(\frac{1}{\eta_j^2} + \eta_j^2\right) + (-1)^{j-1}i\gamma\frac{\partial}{\partial x} \right.$$

$$+ \frac{g_{jj}}{\eta_j^2} |\phi_j|^2 + \frac{2g_{12}}{\eta_1^2 + \eta_2^2} |\phi_{3-j}|^2 \Big] \phi_j + 2\Gamma \frac{\eta_1 \eta_2}{\eta_1^2 + \eta_2^2} \phi_{3-j} \quad (17)$$

where $\phi_j(x, t)$ is a complex wave-function, with the normalization condition $\int_{-\infty}^{\infty} dx |\phi_j(x, t)|^2 = N_j$, and the conserved total number of atoms is $N = N_1 + N_2$. The corresponding transverse widths $\eta_j(x, t)$, are

$$\begin{aligned} \eta_j^4 = & 1 + g_{jj} |\phi_j|^2 + 4g_{12} \frac{\eta_j^4}{(\eta_1^2 + \eta_2^2)^2} |\phi_{3-j}|^2 \\ & + 2\Gamma (-1)^{j-1} \eta_j^3 \eta_{3-j} \frac{\eta_1^2 - \eta_2^2}{(\eta_1^2 + \eta_2^2)^2} \left(\frac{\phi_1^* \phi_2 + \phi_2^* \phi_1}{|\phi_j|^2} \right) \end{aligned} \quad (18)$$

The models (17) and (18) were derived previously by means of a mean-field approximation [24]. Here the Bogoliubov approximation [40] is applied in the Hamiltonian (3), according to which since the condensate state involves the macroscopic occupation of a single state it is appropriate to split the Bose field operator in two terms, the first one describes a macroscopically populated state, defined as the expectation value of the field operator, and the second one takes into account quantum fluctuations about the state condensed. Since the number of atoms in the single-particle condensate wavefunction is large, the quantum fluctuations are negligible and the dimensional reduction [45] of resulting Hamiltonian leads to the mean-field approximation given above. Our results let see the correspondence between quantum field theory and classical field theory. Besides, these suggest that the models obtained by means of Glauber coherent state are indeed an equivalent tool to the Bogoliubov approximation in research of BECs at zero temperature. In the symmetric case, when the effective nonlinearity coefficients for the intra- and inter-species interactions are equal, i.e., $g_{11} = g_{22} = g_{12} \equiv g$, we have $\eta_1 = \eta_2$ and Eq. (18) takes the form $\eta_1^4 = \eta_2^4 = 1 + g(|\phi_1|^2 + |\phi_2|^2)$. We note that, for the self-repulsive binary BEC $g > 0$, and the self-attractive binary BEC $g < 0$. In that way, the system of two coupled equations (17) represents a generalization of the model introduced earlier for the study of vectorial solitons in two-component BECs [54] and it can be read as [24]

$$\begin{aligned} i \frac{\partial}{\partial t} \phi_j = & \left[-\frac{1}{2} \frac{\partial^2}{\partial x^2} + V(x) + (-1)^{j-1} i\gamma \frac{\partial}{\partial x} \right. \\ & \left. + \frac{1 + (3/2)g(|\phi_1|^2 + |\phi_2|^2)}{\sqrt{1 + g(|\phi_1|^2 + |\phi_2|^2)}} \right] \phi_j + \Gamma \phi_{3-j} \end{aligned} \quad (19)$$

Only if $g(|\phi_1|^2 + |\phi_2|^2) \ll 1$ may the system (19) be considered as one-dimensional. It is possible to construct stationary states using Eq. (19). These states are constructed with the chemical potential μ , by setting $\phi_j(x, t) \rightarrow \phi_j(x) \exp(-i\mu t)$. The resulting equations for stationary fields $\phi_{1,2}$ are compatible with the restriction $\phi_1^*(x) = \phi_2(x)$. In terms of real \mathcal{R} and imaginary \mathcal{I} part we have $\mathcal{R}\{\phi_1\} = \mathcal{R}\{\phi_2\}$, and $\mathcal{I}\{\phi_1\} = -\mathcal{I}\{\phi_2\}$. Thus leading to a single stationary NPSE [24],

$$\mu \Phi = \left[-\frac{1}{2} \frac{d^2}{dx^2} + V(x) + i\gamma \frac{d}{dx} + \frac{1 + (3/2)gN|\Phi|^2}{\sqrt{1 + gN|\Phi|^2}} \right] \Phi + \Gamma \Phi^* \quad (20)$$

where we have defined $\Phi(x) \equiv \sqrt{2/N}\phi_1(x)$, along with the condition mentioned above between the stationary fields $\phi_{1,2}$. The normalization becomes $\int_{-\infty}^{\infty} dx |\Phi(x)|^2 = 1$. In the strong coupling regime $gN|\Phi|^2 \gg 1$, the nonpolynomial nonlinearity reduces to a quadratic form $(3/2)\sqrt{gN}|\Phi|\Phi$. The other hand, in the weakly nonlinear regime $gN|\Phi|^2 \ll 1$ the nonlinearity takes the cubic form $\sim gN|\Phi|^2\Phi$. Where without loss the generality, it is omitted the transverse contribution. In general, the coupled equations (17) are strictly one-dimensional [55], under the condition $\eta_j^4 = 1$ in the system of Eqs. (18), establishing the 1D GPE with SO and Rabi couplings

$$i\frac{\partial}{\partial t}\phi_j = \left[-\frac{1}{2}\frac{\partial^2}{\partial x^2} + V(x) + (-1)^{j-1}i\gamma\frac{\partial}{\partial x} + g_{jj}|\phi_j|^2 + g_{12}|\phi_{3-j}|^2 \right] \phi_j + \Gamma\phi_{3-j} \quad (21)$$

we have omitted the constant contribution of the transverse energy given by 1 (in units of ω_{\perp}). By performing a global pseudo-spin rotation $\sigma_x \rightarrow \sigma_z$ and $\sigma_z \rightarrow \sigma_x$, in the Hamiltonian (2), the model (21) becomes the one that was implemented to studying of nonlinear modes in binary bosonic condensates with nonlinear repulsive interactions and linear SO- and Zeeman-splitting couplings [19].

3. 2D-reduction of the 3D-Hamiltonian

In analogy with the 1D scenario, we use the 3D-Hamiltonian (1) to obtain an effective 2D-Hamiltonian \hat{h}_{2D} and the respective 2D-nonpolynomial Heisenberg equation. The 3D-Hamiltonian is scaled by means of HO length $a_z = \sqrt{\hbar/(m\omega_z)}$, which is established by the trap in the z axis. The length, time, energy and field operators are given in units of a_z , ω_z^{-1} , $\hbar\omega_z$, and $a_z^{3/2}$, respectively. Thus, \hat{H} is given by

$$\hat{H} = \int d\mathbf{r} \left\{ \sum_{j=1,2} \hat{\psi}_j^{\dagger} \left[-\frac{1}{2}\nabla^2 + V(x, y) + \frac{1}{2}z^2 + (-1)^{j-1}i\gamma\frac{\partial}{\partial x} + \pi g_{jj}\hat{\psi}_j^{\dagger}\hat{\psi}_j \right] \hat{\psi}_j + 2\pi g_{12}\hat{\psi}_1^{\dagger}\hat{\psi}_2^{\dagger}\hat{\psi}_2\hat{\psi}_1 + \Gamma \sum_{j=1,2} \hat{\psi}_j^{\dagger}\hat{\psi}_{3-j} \right\} \quad (22)$$

where $j = (1, 2)$ and ψ_j represents the field operators of the two atomic states, $g_{jj} \equiv 2a_{jj}/a_z$, $g_{12} \equiv 2a_{12}/a_z$ are the strengths of the intra- and inter-species interactions. While, $\gamma \equiv k_L a_z$ and $\Gamma \equiv \Omega/(2\omega_z)$ are dimensionless strengths of the SO and Rabi couplings, respectively. The external potential is given by $V(x, y) + z^2/2$. Thus, the many-body Hamiltonian (22) describes a dilute gas of bosonic atoms with SO and Rabi couplings confined in the axial z direction by a HO potential and a generic potential $V(x, y)$ in the transverse (x, y) plane. The bosonic field operators satisfy the commutation relations (6) and (7). The effective 2D-Hamiltonian \hat{h}_{2D} is derived by supposing a Gaussian wave-function for the single-particle ground-state in the z axis,

as in a BEC. Similarly, as it was done above in the 1D case,

$$\hat{\psi}_j(\mathbf{r})|G\rangle = \frac{1}{[\pi\xi_j^2(x, y, t)]^{1/4}} \exp\left[-\frac{z^2}{2\xi_j^2(x, y, t)}\right] \hat{\phi}_j(x, y, t)|G\rangle \quad (23)$$

where $|G\rangle$ is the many-body ground state, while $\xi_j(x, y, t)$ is the axial width for bosonic field operators and $\hat{\phi}_j(x, y, t) = (\hat{\phi}_1(x, y, t), \hat{\phi}_2(x, y, t))^T$ represents the transverse bosonic field operators. By applying this ansatz into the Hamiltonian (22) and neglecting the space derivatives of $\xi_j(x, y, t)$, we obtain the effective Hamiltonian \hat{h}_{2D} as $\hat{H}|G\rangle = \hat{h}_{2D}|G\rangle$, with

$$\begin{aligned} \hat{h}_{2D} = & \int dx dy \left\{ \sum_{j=1,2} \hat{\phi}_j^\dagger \left[-\frac{1}{2} \left(\frac{\partial^2}{\partial x^2} + \frac{\partial^2}{\partial y^2} \right) + V(x, y) \right. \right. \\ & + \frac{1}{4} \left(\frac{1}{\xi_j^2} + \xi_j^2 \right) + (-1)^{j-1} i\gamma \frac{\partial}{\partial x} + \sqrt{\frac{\pi}{2}} \frac{g_{jj}}{\xi_j} \hat{\phi}_j^\dagger \hat{\phi}_j \left. \right] \hat{\phi}_j \\ & \left. + \frac{2\sqrt{\pi}g_{12}}{\sqrt{\xi_1^2 + \xi_2^2}} \hat{\phi}_1^\dagger \hat{\phi}_2^\dagger \hat{\phi}_2 \hat{\phi}_1 + \Gamma \sqrt{\frac{2\xi_1\xi_2}{\xi_1^2 + \xi_2^2}} \sum_{j=1,2} \hat{\phi}_j^\dagger \hat{\phi}_{3-j} \right\} \quad (24) \end{aligned}$$

and by minimizing the energy functional $\langle G|\hat{h}_{2D}|G\rangle$ with respect to $\xi_j(x, y, t)$, we determine the axial widths $\xi_j(x, y, t)$. The ground state $|G\rangle$ is obtained self-consistently from the Hamiltonian (24) and the axial widths ξ_j ,

$$\begin{aligned} \xi_j^4 = & 1 + \sqrt{2\pi}g_{jj}\xi_j \frac{\langle G|\hat{\phi}_j^\dagger \hat{\phi}_j^\dagger \hat{\phi}_j \hat{\phi}_j|G\rangle}{\langle G|\hat{\phi}_j^\dagger \hat{\phi}_j|G\rangle} + 4\sqrt{\pi}g_{12} \frac{\xi_j^4}{(\xi_1^2 + \xi_2^2)^{3/2}} \frac{\langle G|\hat{\phi}_1^\dagger \hat{\phi}_2^\dagger \hat{\phi}_2 \hat{\phi}_1|G\rangle}{\langle G|\hat{\phi}_j^\dagger \hat{\phi}_j|G\rangle} \\ & + \sqrt{2}\Gamma(-1)^{j-1}\xi_j^{5/2}\xi_{3-j}^{1/2} \frac{\xi_1^2 - \xi_2^2}{(\xi_1^2 + \xi_2^2)^{3/2}} \frac{\langle G|(\hat{\phi}_1^\dagger \hat{\phi}_2 + \hat{\phi}_2^\dagger \hat{\phi}_1)|G\rangle}{\langle G|\hat{\phi}_j^\dagger \hat{\phi}_j|G\rangle} \quad (25) \end{aligned}$$

3.1. 2D-nonpolynomial Heisenberg equation

By means of the 2D-Hamiltonian \hat{h}_{2D} and the Heisenberg equation $i\partial_t \hat{\phi}_j = [\hat{\phi}_j, \hat{h}_{2D}]$, we derive the 2D-nonpolynomial Heisenberg equation,

$$\begin{aligned} i\frac{\partial}{\partial t} \hat{\phi}_j = & \left[-\frac{1}{2} \left(\frac{\partial^2}{\partial x^2} + \frac{\partial^2}{\partial y^2} \right) + V(x, y) + \frac{1}{4} \left(\frac{1}{\xi_j^2} + \xi_j^2 \right) + (-1)^{j-1} i\gamma \frac{\partial}{\partial x} \right. \\ & \left. + \sqrt{2\pi} \frac{g_{jj}}{\xi_j} \hat{\phi}_j^\dagger \hat{\phi}_j + \frac{2\sqrt{\pi}g_{12}}{\sqrt{\xi_1^2 + \xi_2^2}} \hat{\phi}_{3-j}^\dagger \hat{\phi}_{3-j} \right] \hat{\phi}_j + \Gamma \sqrt{\frac{2\xi_1\xi_2}{\xi_1^2 + \xi_2^2}} \hat{\phi}_{3-j} \quad (26) \end{aligned}$$

which must be solved self-consistently by using the many-body quantum state of the system $|S\rangle$ in the equations of the transverse widths ξ_j . So in the system (25) we need changing the ground state by the many-body quantum state, i.e. $|G\rangle \rightarrow |S\rangle$. When the many-body state $|S\rangle$ coincides with the Glauber coherent state $|GCS\rangle$ [48, 49], such that, $\hat{\phi}_j(x, y, t)|GCS\rangle = \phi_j(x, y, t)|GCS\rangle$, the 2D-nonpolynomial Heisenberg equation becomes 2D-NPSE describing a BEC with SO and Rabi couplings in a mean-field approximation

$$i\frac{\partial}{\partial t} \phi_j = \left[-\frac{1}{2} \left(\frac{\partial^2}{\partial x^2} + \frac{\partial^2}{\partial y^2} \right) + V(x, y) + \frac{1}{4} \left(\frac{1}{\xi_j^2} + \xi_j^2 \right) + (-1)^{j-1} i\gamma \frac{\partial}{\partial x} \right]$$

$$+ \sqrt{2\pi} \frac{g_{jj}}{\xi_j} |\phi_j|^2 + \frac{2\sqrt{\pi}g_{12}}{\sqrt{\xi_1^2 + \xi_2^2}} |\phi_{3-j}|^2 \Big] \phi_j + \Gamma \sqrt{\frac{2\xi_1\xi_2}{\xi_1^2 + \xi_2^2}} \phi_{3-j} \quad (27)$$

where $\phi_j(x, y, t)$ is a complex wave-function, with normalization $\int_{-\infty}^{\infty} dx dy |\phi_j(x, y, t)|^2 = N_j$, and the conserved total number of atoms is $N = N_1 + N_2$. The corresponding axial widths $\xi_j(x, t)$, are

$$\begin{aligned} \xi_j^4 = & 1 + \sqrt{2\pi}g_{jj}\xi_j |\phi_j|^2 + 4\sqrt{\pi}g_{12} \frac{\xi_j^4}{(\xi_1^2 + \xi_2^2)^{3/2}} |\phi_{3-j}|^2 \\ & + \sqrt{2}\Gamma(-1)^{j-1} \xi_j^{5/2} \xi_{3-j}^{1/2} \frac{\xi_1^2 - \xi_2^2}{(\xi_1^2 + \xi_2^2)^{3/2}} \left(\frac{\phi_1^* \phi_2 + \phi_2^* \phi_1}{|\phi_j|^2} \right) \end{aligned} \quad (28)$$

The system of coupled 2D-nonpolynomial Schrödinger equations (27), along with the equations (28) is derived for the first time in this work. In the symmetric case, when the strengths of the nonlinear interactions between different atomic states are equal, $g_{11} = g_{22} = g_{12} \equiv g$, we have $\xi_1^4 = \xi_2^4 \equiv \xi^4$. The Eqs. (28) taking the form $\xi^4 = 1 + \sqrt{2\pi}g\xi(|\phi_1|^2 + |\phi_2|^2)$. A binary BEC is self-attractive while $g < 0$, and it is self-repulsive when $g > 0$. This equation has exact solutions given by Cardano formula [27, 56]. In analogy with the 1D case, stationary solutions may be sought as $\phi_j(x, y, t) \rightarrow \phi_j(x, y) \exp(-i\mu t)$ with the restriction $\phi_1^*(x, y) = \phi_2(x, y)$. These stationary solutions were studied in [27]. The model (27) is strictly two-dimensional under the condition $\xi_j^4 = 1$ in the system of equations (28). By omitting the constant contribution of the axial energy $1/2$ (in units of ω_z), we get the 2D GPE with SO and Rabi couplings

$$\begin{aligned} i \frac{\partial}{\partial t} \phi_j = & \left[-\frac{1}{2} \left(\frac{\partial^2}{\partial x^2} + \frac{\partial^2}{\partial y^2} \right) + V(x, y) + (-1)^{j-1} i \gamma \frac{\partial}{\partial x} \right. \\ & \left. + \sqrt{2\pi}g_{jj} |\phi_j|^2 + \sqrt{2\pi}g_{12} |\phi_{3-j}|^2 \right] \phi_j + \Gamma \phi_{3-j} \end{aligned} \quad (29)$$

4. Numerical results

We study the ground state of SO coupling BECs by solving numerically the stationary 1D NPSE (20) and the stationary 1D GPE obtained from (21) for $g_{jj} = g_{12} \equiv g$, along with the condition $\phi_1^*(x) = \phi_2(x)$ and setting $\Phi(x) \equiv \sqrt{2/N} \phi_1(x)$. The numerical results are achieved using a split-step Crank-Nicolson method with imaginary time propagation [57]. The imaginary time propagation ($t \rightarrow -it$) does not preserve the normalization, because the time evolution operator is not unitary. To fix the normalization of the wave function we need to includes the restoration of the normalization after each operation of Crank-Nicolson method, just as in a BEC with a single component [57]. This procedure is possible because the model given in equation (20) represents a single 1D NPSE. In a more general case, the restoration of the normalization of the two equations given by the generalized 1D NPSE (19) could be implemented according the approaches outlined in [58]. Thus, we split the stationary 1D NPSE (20), such that the derivative terms (provided by the kinetic energy and the SO term), the contribution of HO potential

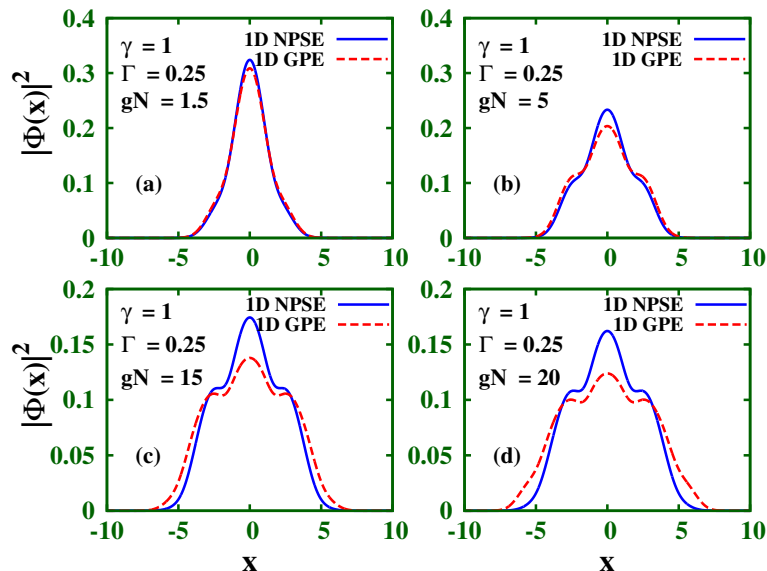


Figure 1. (Color online) Density of a self-repulsive SO and Rabi coupled BEC under axial harmonic confinement given by $V(x) = x^2/18$. We set the SO coupling $\gamma = 1$, the Rabi coupling $\Gamma = 0.25$, and four values of the nonlinearity strength gN , panels (a)-(d). The solid line depicts the density predicted by the 1D NPSE (20) and the dashed line represents the prediction of the stationary 1D GPE obtained by starting from (21). Lengths are measured in units of the transverse confinement radius $a_{\perp} = \sqrt{\hbar/(m\omega_{\perp})}$.

and the nonpolynomial nonlinearity were discretized and implemented as it has been presented in [57]. The term associated with the Rabi coupling was handled by means of the adaptation of the numerical method implemented to obtaining the ground state of atomic-molecular BECs [59]. In a similar way it was solved the 1D GPE through of the respective modification of the nonpolynomial contribution. The spatial and time steps employed in the present work are $\Delta x = 0.01$ and $\Delta t = 0.00025$, respectively. The input wave-function is the known normalized Gaussian $\Phi = \pi^{-1/4} \exp(-x^2/2)$.

We start the study of the ground state structure of the repulsive ($g > 0$) SO and Rabi coupled binary BEC in the presence of a HO axial trap with frequency ω_x , and anisotropy $\lambda \equiv \omega_x/\omega_{\perp}$, such that $V(x) = (\lambda^2/2)x^2$. In Figure 1 (a)-(d) we plot the numerical results of the density profile $|\Phi(x)|^2$ as a function of axial coordinate x . We use $\lambda = 1/3$, the SO coupling $\gamma = 1$, the Rabi coupling $\Gamma = 0.25$, and four values of the nonlinearity strength gN . Our findings show that for the constant values of γ and Γ and increasing the repulsive nonlinearity, the density profile expands and it decreases its height displaying several local maxima (see the right top and the bottom panels in Figure 1). We compare the results of 1D NPSE (20) with the stationary 1D GPE obtained starting from the model (21). The density reduction with the increase of gN is faster in the 1D GPE respect to the 1D NPSE. In the weakly nonlinear regime $gN|\Phi(x)|^2 \ll 1$ both models match very good each other. This fact can be verified in the Table 1 with the values of $gN|\Phi(x=0)|^2$.

Table 1. Values of $gN|\Phi(x=0)|^2$ in a self-repulsive binary BEC with SO and Rabi couplings for the 1D NPSE and the 1D GPE.

gN	1.5	5	15	20
$gN \Phi(x=0) ^2_{NPSE}$	0.486	1.167	2.615	3.243
$gN \Phi(x=0) ^2_{1D\ GPE}$	0.463	1.018	2.068	2.477

It is also relevant analyzing the self-attractive ($g < 0$) SO and Rabi coupled BEC. Now, our aim is investigate effects of gN on the bright solitons. In order to obtaining self-focusing nonlinear waves, we solve numerically the 1D NPSE (20) and the stationary 1D GPE obtained from (21) with $V(x) = 0$ and $g < 0$. In Figure 2 (a)-(d) we plot the density profile $|\Phi(x)|^2$ as a function of axial coordinate x for the bright solitons, with $gN = -0.5$, the Rabi coupling $\Gamma = 0.5$, and four values of SO coupling γ . Interesting issues are the change of the shape of the soliton and the decreasing in the density with the increasing of γ . The results demonstrate that the interplay of the SO and Rabi couplings produces conspicuous sidelobes on the density profile of the bright solitons. Salasnich and co-workers [24], demonstrate an increase of soliton's height and the compression of density profile for a constant γ value and the increase of Γ . For a constant value of Rabi coupling Γ and the increasing of the SO coupling γ , we shown that it is possible to obtaining a decrease in the density profile without a compression of the soliton. The agreement between the 1D NPSE and the 1D GPE is extremely good, and both

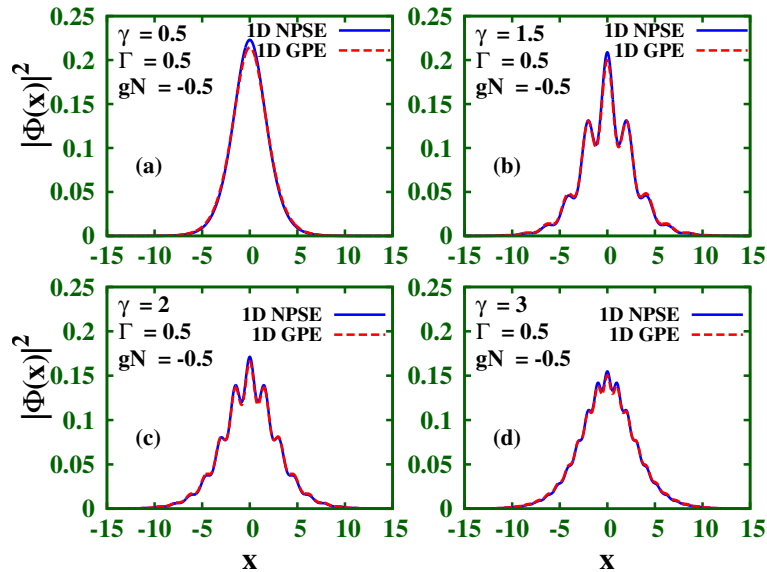


Figure 2. (Color online) Density profile of a self-attractive SO and Rabi coupled BEC without axial confinement, $V(x) = 0$. We use the nonlinearity strength $gN = -0.5$, the Rabi coupling $\Gamma = 0.25$, and four values of the SO coupling γ , panels (a)-(d). The solid line is the solution given by the 1D NPSE (20), and the dashed line represents the prediction of the stationary 1D GPE given from (21). Lengths are measured in units of the transverse confinement radius $a_{\perp} = \sqrt{\hbar/(m\omega_{\perp})}$.

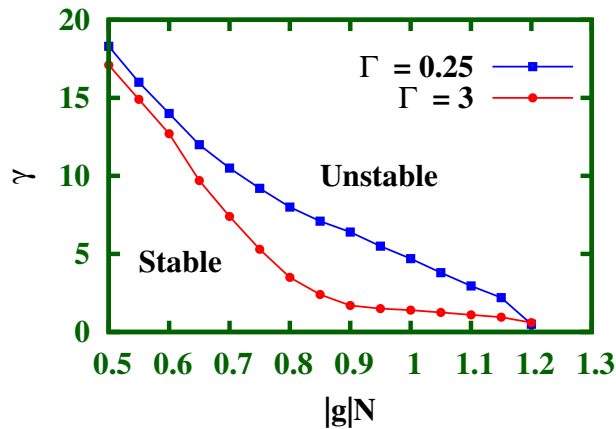


Figure 3. (Color online) Stability diagram of bright solitons in the SO and Rabi coupled BEC. The SO coupling γ versus the nonlinearity strength $|g|N$ for two different values of the Rabi coupling Γ , in dimensionless form.

models predict the existence of self-trapped matter-wave solitons as it is shown in the overlapping of the plots in Figure 2. This can be understood since the 1D NPSE with $gN = -0.5$ becomes effectively 1D. However, it is worth noting, contrary to the 1D GPE, the 1D NPSE predicts the instability by collapse. Now, we analyze some aspects of the collapse in the SO and Rabi couplings BECs by means of the 1D NPSE. It is known that for a self-attractive condensate without SO-coupling and/or with Rabi coupling, the model (20) with $V(x) = 0$ predicts the existence of bright solitons only for $-4/3 < gN < 0$ [54]. By solving the Eq. (20) for bright solitons in the absence of the axial confinement, we plot in Figure 3 the positive SO coupling ($\gamma > 0$) as function of the strength $|g|N$ for two different values of Γ . Similar plots exist in the range $0.25 < \Gamma < 3$. With the increasing of the attraction the density profile of the soliton shrinks, and once the strength of the interaction exceeds the critical value of $|g|N$, the condensate becomes so attractive that growth peak height is stopped by inelastic collisions and the system must collapse. We find the critical value $|g|N \simeq 1.2$ beyond which the condensate collapses, and it is not dependent on the Rabi coupling. We verified a reduction of the collapse threshold for bright solitons under the action of the SO and Rabi couplings, initially predicted in [24]. The 1D NPSE (20) gives rise to the collapse of the condensate, when the density of the condensate in the denominator of the nonlinear term reaches a critical value $|\Phi|^2 = (|g|N)^{-1}$ [24, 45]. This implies that the effective nonpolynomial nonlinearity in the 1D NPSE is quite essential compared with the cubic nonlinearity in 1D GPE where there is no collapse. The reduction in the SO coupling caused by the increasing of the strength of the interaction is reflected in the density of the soliton as an increasing in the real component of the wave function and decreasing in the imaginary one, together with decreasing in the oscillations in both parts of the wave function. Now we consider the possible origin of the unstable region in Figure 3. To achieve this purpose we fix the values of Rabi coupling Γ and the strength of interaction $|g|N$,

and we increase the SO coupling γ . Above a critical value determined by the plots in Figure 3, the oscillations set by the SO coupling becomes unstable the condensate and it is destroyed. This unstable region could be experimentally analyzed by means of a recently technique implemented in [60]. Here it has been proposed a scheme for controlling SO-coupling between two hyperfine ground states in a binary BEC through a fast and coherent modulation of the Raman laser intensities. The above results also apply at $\gamma < 0$. In that case we have $x \rightarrow -x$ in 1D NPSE (20) and the diagram of Figure 3 is symmetric.

5. Summary and outlook

We have analyzed the 1D and 2D dimensional reduction of a binary bosonic quantum field theory in which the two components are coupled by the nonlinear inter-atomic interactions and the SO and Rabi couplings. We have derived for the first time, an effective 1D and 2D quantum Hamiltonian with the corresponding effective 1D and 2D nonpolynomial Heisenberg equations, for both self-repulsive and self-attractive inter-atomic interactions. These 1D and 2D models open the door to a new level in the research of interacting gases of bosons with SO and Rabi couplings at finite temperature in reduced dimensions. Recently, dramatic implications were predicted about the effect of the SO coupling on thermal properties of bosonic gases [47], showing thus the amplification of quantum fluctuations induced by the SO coupling. We show the possibility of obtaining two models in a mean-field approximation derived from the quantum field equations in the case in which the many-body quantum state of the system coincides with the Glauber coherent state. Our findings are agree with the system of coupled NPSEs considered in the study of dynamics of BECs with SO and Rabi couplings in one [24] and two dimensions [27]. The numerical results demonstrate the emergence of conspicuous sidelobes on the density profile due to the interplay of SO and Rabi couplings, for both signs of the interaction. The mean-field approximation given by 1D NPSE in repulsive BECs with SO and Rabi couplings shows the relevance of nonlinearity compared to 1D GPE. An interesting result in the 1D NPSE describing self-attractive binary BECs, is the possibility of getting an unstable condensate by fixing the Rabi coupling and the strength of interaction and by increasing of SO coupling. Thus showing a new instability in addition to the existing collapse threshold, established by the strength of interaction.

The effective 1D and 2D models can be used to study the effect of inhomogeneous nonlinearity, as well as general forms of the couplings. One may expect interesting issues with non trivial effects by extending the present analysis for matter-wave vortices. In the absence of two couplings, vortical states in a BEC have been studied by means of 1D [61] and 2D [56] NPSEs.

References

- [1] Lin Y-J, Jiménez-García K, and Spielman I B 2011 Nature (London) **471**, 83
- [2] Zhang J-Y, Ji S-C, Chen Z, Zhang L, Du Z-D, Yan B, Pan G-S, Zhao B, Deng Y-J, Zhai H, Chen S, and J-W Pan 2012 Phys. Rev. Lett. **109**, 115301
- [3] Wang P, Yu Z Q, Fu Z, Miao J, Huang L, Chai S, Zhai H, and Zhang J 2012 Phys. Rev. Lett. **109**, 095301
- [4] Cheuk L W, Sommer A T, Hadzibabic Z, Yefsah T, Bakr W S, and Zwierlein M W 2012 Phys. Rev. Lett. **109**, 095302
- [5] Zhai H 2012 Int. J. Mod. Phys. B **26**, 1230001
- [6] Zheng W, Yu Z-Q, Cui X and Zhai H 2013 J. Phys. B: At. Mol. Opt. Phys. **46**, 134007
- [7] Ho T L and Zhang S Z 2011 Phys. Rev. Lett. **107**, 150403
- [8] Xu X-Q and Han J H 2011 Phys. Rev. Lett. **107**, 200401
- [9] Radic J, Sedrakyan T A, Spielman I B, and Galitski V 2011 Phys. Rev. A **84**, 063604
- [10] Zhou X F, Zhou J, and Wu C J 2011 Phys. Rev. A **84**, 063624
- [11] Sinha S, Nath R, and Santos L 2011 Phys. Rev. Lett. **107**, 270401
- [12] Hu H, Ramachandhran B, Pu H, and Liu X-J 2012 Phys. Rev. Lett. **108**, 010402
- [13] Ramachandhran B, Opanchuk B, Liu X-J, Pu H, Drummond P D, and Hu H 2012 Phys. Rev. A **85**, 023606
- [14] Wen L, Sun Q, Wang H Q, Ji A C, and Liu W M 2012 Phys. Rev. A **86**, 043602
- [15] Wang C, Gao C, Jian C M, and Zhai H 2010 Phys. Rev. Lett. **105**, 160403
- [16] Ruokokoski E, Huhtamäki J A M, and Möttönen M 2012 Phys. Rev. A **86**, 051607(R)
- [17] Li Y, Pitaevskii L P, and Stringari S 2012 Phys. Rev. Lett. **108**, 225301
- [18] Barnett R, Powell S, Gra T, Lewenstein M, and Das Sarma S 2012 Phys. Rev. A **85**, 023615
- [19] Zezyulin D A, Driben R, Konotop V V, and Malomed B A 2013 Phys. Rev. A **88**, 013607
- [20] Deng Y, Cheng J, Jing H, Sun C-P, and Yi S 2012 Phys. Rev. Lett. **108**, 125301
- [21] Xu Y, Zhang Y, and Wu B 2013 Phys. Rev. A **87**, 013614
- [22] Achilleos V, Frantzeskakis D J, Kevrekidis P G, and Pelinovsky D E 2013 Phys. Rev. Lett. **110**, 264101
- [23] Kartashov Y V, Konotop V V, and Abdullaev F Kh 2013 Phys. Rev. Lett. **111**, 060402
- [24] Salasnich L and Malomed B A 2013 Phys. Rev. A **87**, 063625
- [25] Sakaguchi H, Li B, and Malomed B A 2014 Phys. Rev. E **89**, 032920
- [26] Lobanov V E, Kartashov Y V, and Konotop V V 2014 Phys. Rev. Lett. **112**, 180403
- [27] Salasnich L, Cardoso W B, and Malomed B A 2014 Phys. Rev. A **90**, 033629
- [28] Sakaguchi H. and Li B 2013 Phys. Rev. A **87**, 015602
- [29] Fetter A L 2014 Phys. Rev. A **89**, 023629
- [30] Fetter A L 2015 J. Low Temp. Phys. **180**, 37
- [31] Cheng Y S, Tang G H, and Adhikari S K 2014 Phys. Rev. A **89**, 063602
- [32] He P-S 2013 Eur. Phys. J. D **67**, 48
- [33] He P-S, You W-L, and Liu W-M 2013 Phys. Rev. A **87**, 063603
- [34] Gautam S and Adhikari S K 2015 Laser Phys. Lett. **12** 045501
- [35] Gautam S and Adhikari S K 2015 Phys. Rev. A **91** 063617
- [36] Mardonov Sh, Sherman E Ya, Muga J G, Wang Hong-Wei, Ban Yue, and Chen Xi 2015 Phys. Rev. A **91**, 043604
- [37] Zhang D-W, Fu L-B, Wang Z D, and Zhu S-L 2012 Phys. Rev. A **85**, 043609
- [38] Garcia-March M A, Mazzarella G, Dell'Anna L, Juliá-Díaz B, Salasnich L, and Polls A 2014 Phys. Rev. A **89**, 063607
- [39] Cornish S L, Thompson S T, and Wieman C E 2006 Phys. Rev. Lett. **96**, 170401
- [40] Dalfovo F, Giorgini S, Pitaevskii L P, and Stringari S 1999 Rev. Mod. Phys. **71** 463
- [41] Eiermann B, Anker Th, Albiez M, Taglieber M, Treutlein P, Marzlin K-P, and Oberthaler M K 2004 Phys. Rev. Lett. **92**, 230401

- [42] Giamarchi T 2004 *Quantum Physics in One Dimension (Great Britain: Oxford University Press)*
- [43] Cazalilla M A, Citro R, Giamarchi T, Orignac E, and Rigol M 2011 *Rev. Mod. Phys.* **83** 1405
- [44] Muñoz Mateo A, and Delgado V 2008 *Phys. Rev. A* **77**, 013617
- [45] Salasnich L, Parola A, and Reatto L 2002 *Phys. Rev. A* **65**, 043614
- [46] Sinha S and Santos L 2007 *Phys. Rev. Lett.* **99**, 140406
Muruganandam P and Adhikari S K 2012 *Laser Phys.* **22**, 813-20
Chiquillo Emerson 2014 *Laser Phys.* **24**, 085502
- [47] Liao R, Huang Z-G, Lin X-M, and Fialko O 2014 *Phys. Rev. A* **89**, 063614
- [48] Barbiero L and Salasnich L 2014 *Phys. Rev. A* **89**, 063605
- [49] Salasnich L 2015 *Quodons in Mica (Springer series in materials science vol 221 Discrete bright solitons in Bose-Einstein condensates and dimensional reduction in quantum field theory)* ed Archilla J F R , Jiménez N, Sánchez-Morcillo V J, and García-Raffi L M (Springer International Publishing)
- [50] Salasnich L 2014 *Quantum Physics of Light and Matter. A Modern Introduction to Photons, Atoms and Many-Body Systems (Cham: Springer)* p. 167
- [51] Stoof H T C, Gubbels K, Dickerscheid D 2009 *Ultracold Quantum Fields (Berlin: Springer)* p. 131
- [52] Rogel-Salazar J, Choi S, New G H C, and Burnett K 2004 *J. Opt. B: Quantum Semiclass. Opt.* **6** R33-R59
- [53] Glauber R 1963 *Phys. Rev.* **131**, 2766
Zhang W-M, Feng D H, and Gilmore R 1990 *Rev. Mod. Phys.* **62**, 867
- [54] Salasnich L. and Malomed B A 2006 *Phys. Rev. A* **74**, 053610
- [55] Achilleos V, Stockhofe J, Kevrekidis P G, Frantzeskakis D J, and Schmelcher P 2013 *Eur. Phys. Lett.* **103**, 20002
- [56] Salasnich L and Malomed B A 2009 *Phys. Rev. A* **79**, 053620
- [57] Muruganandam P and Adhikari S K 2009 *Comput. Phys. Commun.* **180**, 1888
- [58] Bao W and Cai Y 2015 *Siam J. Appl. Math.* **75**, 492
Bao W and Cai Y 2011 *East Asia Journal on Applied Mathematics* **1**, 49-81
- [59] Jiang W, Wang H, and Li X 2013 *Comput. Phys. Commun.* **184**, 2396
- [60] Zhang Y, Chen G, and Zhang C 2013 *Sci. Rep.* **3**, 1937
Lian J, Yu L, Liang J-Q, Chen G, and Jia S 2013 *Sci. Rep.* **3** 3166
Jiménez-García K, LeBlanc L J, Williams R A, Beeler M C, Qu C, Gong M, Zhang C, and Spielman I B 2015 *Phys. Rev. Lett.* **114**, 125301
- [61] Salasnich L, Malomed B A, and Toigo F 2007 *Phys. Rev. A* **76**, 063614